Copolymerization Behaviour and Structure of Styrene and Polymerizable Surfactants in Three-Component Cationic Microemulsion

Michael Dreja,[†] Wim Pyckhout-Hintzen,[‡] and Bernd Tieke*,[†]

Institut für Physikalische Chemie, Universität zu Köln, Luxemburger Strasse 116, D-50939 Köln, Germany, and Institut für Festkörperforschung, Forschungszentrum Jülich (KFA), Postfach 1913, D-52425 Jülich, Germany

Received July 31, 1997; Revised Manuscript Received October 31, 1997

ABSTRACT: The copolymerization and structural properties of the ternary o/w-microemulsions formed from water, styrene and (11-(acryloyloxy)undecyl)trimethylammonium bromide or (2-(methacryloyloxy)-ethyl)dodecyldimethylammonium bromide as cationic polymerizable surfactants are investigated. The two surfactants contain the polymerizable group either at the hydrophobic tail (T-type) or at the hydrophilic head group (H-type) and form micellar structures in aqueous solution. Upon addition of styrene, transparent, globular o/w-microemulsions are formed without any addition of a cosurfactant. The microemulsions can be polymerized upon γ-irradiation at room temperature. Copolymers with completely different morphology are obtained. With styrene and the T-type surfactant, very small nanolatex particles are formed similar to microemulsion polymerization of styrene and nonpolymerizable surfactants. In contrast, copolymerization of styrene and the H-type surfactant monomer results in transparent nanogels with high water content. The structure of the micelles and o/w-microemulsions before and after polymerization was studied using small-angle neutron scattering (SANS), while the copolymer structure was analyzed using NMR and IR spectroscopy. SANS experiments show that in the water/H-type surfactant/styrene system the overall structure of the parent microemulsion is largely preserved whereas in the T-type system distinct changes are observed. Structure models are presented which take into account the different properties of the resulting polymer materials at both a macroscopic and a microscopic length scale.

Introduction

Self-organized surfactant systems like micelles or microemulsions are useful as reaction media for controlled formation of colloid materials, as, for example, organic and inorganic nanoparticles. During the past few years, tremendous advances has been reported on polymer synthesis in microemulsion.[1−3] The goal of polymerization in microemulsion is to control the structural properties of the resulting polymers on a mesoscopic scale. Polymerization of the oil component in globular o/w-microemulsion leads to ultrasmall latex particles with narrow particle size distribution.[4−6] Since it has been shown that the use of cosurfactants such as long chain alcohols may cause chain transfer during polymerization,[7] the long-known systems with four or more components[8−10] have been sucessfully replaced by three-component systems consisting merely of surfactant, oil, and water.[11−15] A typical example is the polymerization of styrene in water using the cationic single tail surfactant dodecyltrimethylammonium bromide (DTAB). Also, styrene polymerization in nonaqueous mixtures has been reported.[16] The surface properties of the polystyrene latex particles can be controlled via copolymerization of hydrophilic comonomers such as acrylic acid, which simultaneously act as cosurfactants in the parent microemulsion.[17−20] The formation of particles with a core−shell morphology was observed, but most of the systems are fragile and a destabilization of the original structure during the polymerization process is often observed. Also, the addition of a comonomer increases the degree of freedom of the system, which complicates the phase behavior considerably.

The polymerization of bicontinous microemulsions has also been widely studied.[21−25] In most cases, the parent microemulsion structure was not completely maintained. The polymerization resulted in porous materials with a size range of 0.2−3 μm. In some studies, primary particles of spherical shape occurred, which later aggregated to macroscopically porous gel structures. A rheological study by Antonietti and Hentze[26] indicated that during polymerization in a bicontinous microemulsion several phase transitions may occur. It was shown that the initial polymer destabilizes the bicontinous phase so that the morphology of the resulting polymer does not necessarily reflect the original structure. Nevertheless, Chieng et al. reported on the control of such structures via a change of the surfactant chain length[27] and on the use of the resulting materials as membranes.[28]

Recently polymerizable surfactants were used in microemulsion polymerization. Polymerization has been studied in bicontinous systems[29−31] as well as w/o[32] and o/w-microemulsions.[33] Polymerizable surfactants have the advantage over nonpolymerizable surfactants that the templating effect of the amphiphilic interface may be better preserved during polymerization. Upon copolymerization of the polymerizable surfactant (11-(acryloyloxy)undecyl)trimethylammonium bromide (AUTMAB) and styrene in ternary globular o/w-systems, very small functionalized nanolatex particles were formed, which could successfully be redispersed in polar media. This suggested a core−shell structure of the particles, in which the surfactant forms the hydrophilic particle shell. However, the size of the particles was considerably greater than the typical droplet size of

* Author to whom correspondence should be addressed.
[†] Universität zu Köln.
[‡] Forschungszentrum Jülich (KFA).

S0024-9297(97)01153-4 CCC: $15.00
Published on Web 01/27/1998

microemulsions, indicating that simple fixation of the original structure was not possible.[33]

In the present paper, we want to elucidate in more detail how the molecular structure of polymerizable cationic surfactants determines the morphology of the resulting copolymer in microemulsion copolymerization. Therefore, two polymerizable surfactants bearing functional groups in different positions have been used to prepare o/w-microemulsion with styrene. AUTMAB is a so-called T-type surfactant which has its polymerizable moiety at the hydrophobic alkyl tail end, and (2-(methacryloyloxy)ethyl)dodecyldimethylammonium bromide (MEDDAB) is an H-type surfactant and contains the polymerizable moiety near to the hydrophilic head group. The two molecular structures are shown as follows:

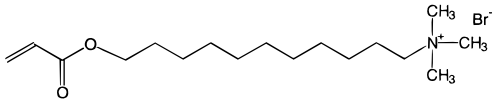

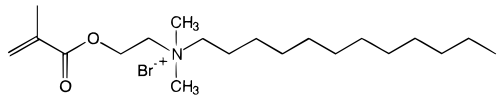

In order to investigate the microstructure of micelles and microemulsions containing water, styrene, and one of the two polymerizable surfactants, small-angle neutron scattering (SANS) experiments were carried out before and after polymerization. Polymerization was initiated using ^{60}Co γ-radiation which is advantageous for microemulsions, because no additional initiator component is needed and the polymerization can be carried out at room temperature. The resulting copolymers were examined by spectroscopic methods. Finally, the results will be discussed in relation to the phase and polymerization behavior of the two different types of surfactant monomers used, which is already known to determine the properties of surfactant homopolymers.

Experimental Section

Materials. Styrene (Aldrich) was freshly distilled before use in order to remove the inhibitor and oligomeric impurities. Hydroquinone (Merck) was used as received. Milli-Q_{PLUS} water was used for all experiments. Deuterium oxide (Fluka, >99.8%) was used when samples for the scattering experiments were prepared. The polymerizable surfactants were prepared according to the literature.[34,35] The properties of AUTMAB have been described previously.[33]

For purification MEDDAB was recrystallized three times from acetone containing a small amount of dry ethanol. A white crystalline solid with a melting point of 83 °C (DSC) was found in accordance with the literature. ^{1}H-NMR: ($CDCl_3$, 300 MHz, δ in ppm) 6.09d (*trans* CH_2═C, 1H), 5.62d (*cis* CH_2═C, 1H), 4.62t ($COOCH_2$, 2H), 4.13m (α-CH_2−N, 2H), 3.58t (N−α-CH_2, 2H), 3.47s ($N(CH_3)_2$, 6H), 1.71m (N−β-H_2, 2H), 1.14−1.4m (−$(CH_2)_9$−, 18H), 0.83t (−CH_3, 3H). Surface tension measurements were carried out in aqueous solution using the Wilhelmy plate method (Krüss Digital-Tensiometer K 10) at a temperature of (25 ± 0.1) °C. Cmc values of 1.74×10^{-2} and 4.0×10^{-3} mol/L were found for AUTMAB and MEDDAB, respectively.

Methods. The single phase regions of the microemulsions at 25 and 60 °C were determined visually from their transparency. The composition was changed by titrating styrene into water-surfactant mixtures in screw-capped glass tubes. Each sample was thoroughly homogenized using a Vortex mixer and thermostated in a water bath. In order to determine the phase diagram at 60 °C styrene was used, to which a few parts per million of hydroquinone had been added in order to prevent a thermal polymerization.

Polymerization in microemulsion was performed in closed glass vessels at 23 °C. The transparent samples were treated with ultrasonic irradiation shortly before use in order to remove small gas bubbles. No attempts were made to remove dissolved oxygen, because a purging of the samples with an inert gas would have been accompanied by a partial evaporation of the styrene from the microemulsion. ^{60}Co-γ-radiation was used for the polymerization. The dose rate was 56.5 krad/h or 565 Gy/h (1 rad = 10^{-5} J/g = 0.01 J/kg = 0.01 Gy). The overall monomer coversion was determined gravimetrically after leaching out the resulting polymer material in both toluene and water.

Particle size and size distribution were determined with a Nicomp C 370 particle sizer. For the measurement, γ-irradiated samples were quenched with hydroquinone, diluted and kept at constant temperature of (25 ± 0.1) °C. The measured correlation functions were fitted with a Gaussian distribution function for the relaxation times. The resulting diffusion coefficients were converted into the corresponding hydrodynamic particle diameters and a distribution width using the Stokes equation, while for the solvent the viscosity of water was used.

^{1}H-NMR spectroscopy was carried out using a 300 MHz Bruker AC 300 machine. FTIR spectra were taken using a Perkin-Elmer Paragon 1000 spectrometer.

Small-Angle Neutron Scattering (SANS). SANS experiments were performed at the KWS1−instrument in Forschungszentrum Jülich GmbH (KFA) using the FRJ-2 research DIDO-reactor (23 MW). The neutron wavelength λ was 7 Å with $\Delta\lambda/\lambda$ = (0.21 ± 0.02) and scattered intensities were measured over a scattering vector range $\boldsymbol{q}$ from 0.006 to 0.16 Å^{-1} using two or three different sample-to-detector distances (2 m, 4 m, 8 m); $|\boldsymbol{q}| = (4\pi/\lambda) \times \sin(\theta/2)$, where θ is the scattering angle. The detection was two-dimensional in 64 × 64 channels of 0.8 cm width.

The samples were put in quartz cells of 1 or 2 mm path length tightly closed with Teflon stoppers. All measurements were performed at a constant temperature of 23 °C. Scattering from the samples was corrected for sensitivity and dark current of the detector, solvent, and empty cell scattering and normalized to sample thickness and transmission. The resulting intensities were radially averaged and placed on an absolute scale using a secondary Lupolen-standard and software provided by the neutron facility. The absolute cross sections are shown as open points in Figures 2, 3, and 7. The solid lines in these figures are calculated as described below.

SANS Analysis. SANS analysis was carried out in order to determine size, shape, and polydispersity of the micelles and microemulsions. For contrast enhancement, D_2O was used in the scattering experiments instead of H_2O. Generally, the observed differential scattering cross section, $d\Sigma(\boldsymbol{q})/d\Omega = I(\boldsymbol{q})$, of a dispersion of N_p monodisperse particles is given by[36,37]

$$I(\boldsymbol{q}) = A n_p P(\boldsymbol{q})\, S(\boldsymbol{q}) + B \qquad (1)$$

where $n_p = N_p/V$ is the number density of particles, $P(\boldsymbol{q})$ is the identical particle form factor for each particle depending on the particle size and shape, $S(\boldsymbol{q})$ is the interparticle structure factor arising from interparticle scattering and depending on interparticle separation and interaction potentials, A is an instrumental constant and B is a background constant that represents incoherent scattering.

Specifying the volume fraction of the dispersed phase ϕ and the scattering length density difference of the samples, $\Delta\rho = (\rho_p - \rho_s)$, in which ρ_p and ρ_s are the scattering length densities of the particle and of the solvent, respectively, eq 1 becomes

$$I(\boldsymbol{q}) = A' \phi\, (\Delta\rho)^2\, P(\boldsymbol{q})\, S(\boldsymbol{q}) + B \qquad (2)$$

If particles exhibit a nonspherical shape or a polydisperse size distribution, a decoupling approximation[38] is appropriate to correctly describe the scattering intensity in an effective

one-component system. The resulting approximate expression assumes that no correlation of particle orientation or size with its position takes place. For the calculation of $S(\boldsymbol{q})$, the particles are redefined as spheres of equivalent volume; polydispersity in the particle size was modeled by a Gaussian size distribution. Eq 2 can thus be rewritten as

$$I(\boldsymbol{q}) = A'\phi(\Delta\rho)^2 P(\boldsymbol{q}) S'(\boldsymbol{q}) + B \tag{3}$$

with

$$S'(\boldsymbol{q}) = 1 + \beta(\boldsymbol{q})\,[S(\boldsymbol{q}) - 1] \tag{4}$$

$$\beta(\boldsymbol{q}) = \langle F(\mathbf{q})\rangle^2/\langle F(\mathbf{q})^2\rangle \tag{5}$$

$F(\boldsymbol{q})$ is the amplitude factor for each particle depending on the particle geometry. For our purpose, $\beta(\boldsymbol{q})$ was set to 1.0 as for perfectly monodisperse particles as is done in the local monodisperse approximation by Pedersen et al.[39] which works better at higher concentrations. In view of the relatively small polydispersity in the radii (see later) and the assumption of a Gaussian distribution function this is expected not to influence the data modeling severely.

In the case of ionic micelles and microemulsions, equally charged particles with repulsive interactions are present. In order to take these charges into account, structure factors are calculated either using an effective hard sphere potential (EHS) with a hard sphere radius r_{hs}, and a hard sphere volume fraction ϕ_{hs} or a screened Coulomb (Yukawa) potential.[40] In our systems, the measured intensity was generally modeled by the Yukawa potential:

$$V(r)/k_b\,T = z^2\,L_b\,\exp[-\kappa\,(r - 2\,r_{hs})]/r(1 + \kappa r_{hs})^2 \quad \text{for } r > 2\,r_{hs} \tag{6}$$

while $V(r)/k_b\,T$ is infinite for $r \le 2\,r_{hs}$.

In eq 6, L_b is the Bjerrum length $L_b = e^2/(4\pi\epsilon\epsilon_0 k_b T)$ and z the number of charges per particle. In this case, the two interaction parameters γ and ξ were introduced in addition to the hard sphere radius r_{hs}, in order to calculate the structure factor $S(\boldsymbol{q})$. $\gamma = z^2\,L_b$ is a measure for interaction strength and $\xi = 1/\kappa = (4\,\pi\,L_b\,N_a\,I)^{1/2}$ is the Debye length, a measure for the characteristic length of the interaction. $S(\boldsymbol{q})$ was then calculated assuming a one-component macroion model (OCM) using either the Percus-Yerwick (PY) closure relation for the Ornstein−Zernike equation in the EHS-case[40] or the mean spherical approximation (MSA) in the case of Yukawa-potential interactions.[41]

Since $S(\boldsymbol{q})$ becomes 1 at infinite dilution, $P(\boldsymbol{q})$ cannot be independently determined. Several particle geometries[42] were tested for calculation of model spectra. The form factor of a homogeneous sphere can be expressed using a first-order spherical Bessel function

$$F_s^2(\boldsymbol{q}, r) = (3\,[\sin(\boldsymbol{q}r) - \boldsymbol{q}r\cos(\boldsymbol{q}r)]/\boldsymbol{q}r^3)^2 \tag{7}$$

The form factor for ellipsoids of revolution with semi axes r, r and ϵr has been derived to be

$$P_e(\boldsymbol{q}, r, \epsilon) = \int_0^{\pi/2} F_s^2\,[\boldsymbol{q}, R_e(r, \epsilon, \alpha)]\,\sin\alpha\,d\alpha \tag{8}$$

$$R_e(r,\epsilon,\alpha) = r(\sin^2\alpha + \epsilon^2\cos^2\alpha)^{1/2} \tag{9}$$

For $\epsilon = 1$ the sphere form factor is retrieved. Standard nonlinear least-squares fitting was used to determine the best parameter set for each sample. The incoherent background scattering due to the presence of hydrogen atoms was considered in the fitting procedure. Model functions were convoluted with a resolution function to correct for smearing due to finite apertures and wavelength distribution. The known volume fraction ϕ of the dispersed phase was used to specify the micelle dimensions via r and ϵ, from which the surfactant and styrene aggregation numbers can be calculated using molecular volumes.[43] In all calculations, nonaggregated surfactant was subtracted and hydration of the head group ions[36] was taken into account. The concentration of the nonaggregated surfactant was assumed to be equal to the cmc.

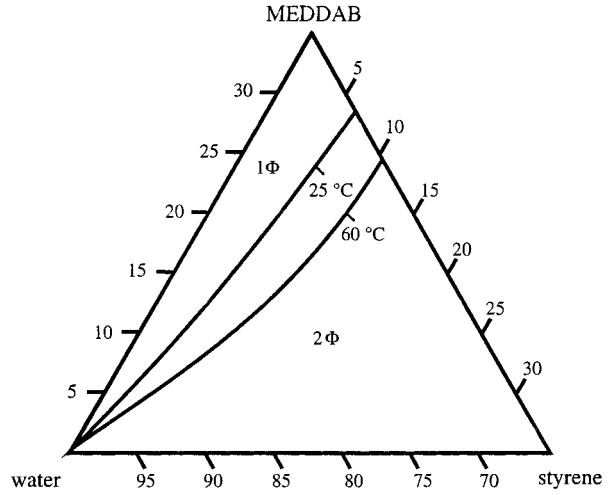

Figure 1. Partial phase diagram of MEDDAB/styrene/water at 25 and 60 °C. The one-phase region (1ϕ) is close to the water-edge in the Gibbs's phase triangle. The lines represent the compositions defining the boundary between one-phase and two-phase regions.

Results and Discussion

Phase Diagrams. In Figure 1, partial phase diagrams of the system water/MEDDAB/styrene at 25 and 60 °C are shown. It can be seen that the ternary mixture forms a single phase microemulsion region near to the water-edge of the diagram. Within the one phase region, the samples are transparent and fluid. With increasing surfactant and/or styrene concentration, the viscosity remarkably increases and the samples become viscous like hair shampoo. Upon an increase of the temperature from 25 to 60 °C the single phase region is extended. The behavior of the system is comparable with water/DTAB/styrene mixtures.[6] Quite a different behavior is found for water/AUTMAB/styrene. As already reported,[33] it shows an inverse temperature dependence of the phase behavior and has a viscosity like water, which probably has its origin in the slightly bipolar structure of AUTMAB originating from the hydrophilic character of the polymerizable acrylate moiety at the end of the alkyl chain. Due to the bipolarity, AUTMAB also exhibits a distinctly higher critical micelle concentration (1.7×10^{-2} mol/L^{-1}) than MEDDAB (4.0×10^{-3} mol/L^{-1}). Hence it can be inferred that the aggregation behavior of MEDDAB with the polymerizable moiety near to the ionic head group is more similar to that of the common *n*-alkyltrimethylammonium halide surfactants than the behavior of AUTMAB.

Structure Studies of Monomeric Systems. Structure studies of aqueous micellar solutions of the two surfactants and ternary o/w-microemulsions were carried out using small-angle neutron scattering (SANS). In parts a and b of Figure 2, the scattering curves are plotted for micellar solutions of MEDDAB and for microemulsions of the water/MEDDAB/styrene system, respectively. The SANS curves of the micellar solutions (Figure 2a) show interaction peaks being characteristic for dispersions of charged spheres. With increasing surfactant concentration, the maximum shifts to higher

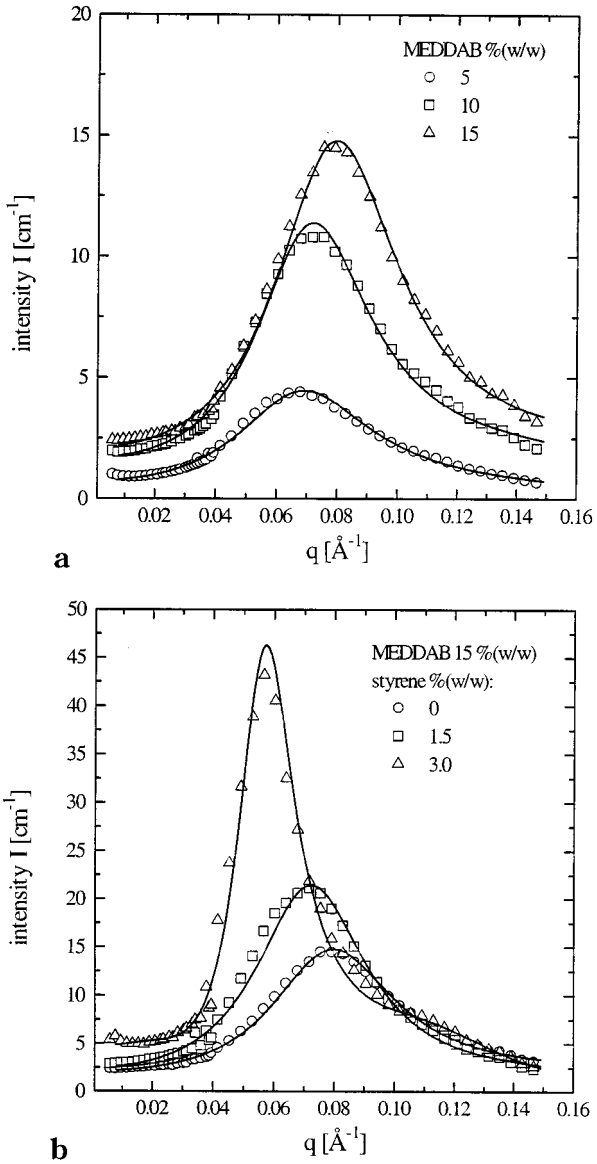

Figure 2. SANS spectra of (a) MEDDAB micelles and (b) microemulsions with styrene at an MEDDAB/water ratio of 15/85% (w/w). Open symbols represent the measured data points, and solid lines are the model intensities.

q values, while the absolute scattering intensity increases. This behavior can be interpreted as a decrease of the interparticle separation with increasing surfactant concentration. Upon the addition of styrene at a constant surfactant/water ratio of 15/85% (w/w), the maximum intensity increases even more (Figure 2b), but the maximum peak position is shifted to lower ***q*** values. This is consistent with a swelling of the micelles due to styrene incorporation leading to the globular o/w-microemulsion.[44] Data were analyzed by comparing the measured spectra with calculated spectra using the equations described in the experimental part. The fitting parameters are compiled in Table 1. As can be seen, the micelles are most accurately described by assuming a nearly spherical shape and a semimajor axis r of 28−30 Å. The styrene-containing microemulsions both exhibit droplets with a larger semimajor axis of 32 and 35 Å, respectively. Also, it is not possible to fit a suitable model intensity without assuming that the shape of the droplets becomes more and more ellipsoidal (Table 1). The axial ratio ϵ of the micelles only slightly increases from 1.1 for a 5% (w/w) aqueous solution to 1.2 for a 15% (w/w) solution. If 3% (w/w) styrene are added to a 15/85 surfactant/water mixture, ϵ considerably increases to a value of 3.4 which means that the semiminor axis of the ellipsoid is about 140 Å. Thus the higher viscosity of the resulting microemulsions can be explained by a structural rearrangement of the spheres into prolate ellipsoidal droplets. Consequently, the aggregation number increases as well. The results suggest that the addition of styrene alters the mean curvature of the interfacial surfactant film and leads to flatter aggregates. Indeed, a high droplet polydispersity may cause similar scattering spectra as the elliptical monodisperse particles, but for our systems the model calculations for polydisperse spheres did not produce any suitable fitting curves. A possible explanation for the observed behavior results from the influence of the polymerizable moiety near to the ionic head group. In the micellar solution, the polar methacrylate moiety should preferably be located in the interfacial layer near to the water phase. Upon the addition of styrene, which is incorporated into the droplet core, the polymerizable group rather tends toward the oil phase and thus acts as a small second surfactant tail. It is known from the literature that surfactants with polar headgroups can form elongated aggregates if they are mixed with a second hydrophobic polar compound at comparable concentrations.[45]

In parts a and b of Figure 3, the scattered intensities are plotted for aqueous micellar solutions of AUTMAB and for microemulsions of the water/AUTMAB/styrene system, respectively. The differences between the SANS spectra of the AUTMAB and the MEDDAB systems are obvious: For equivalent surfactant concentrations, all

Table 1. Parameters from SANS Spectra Analysis[a]

surfactant	% (w/w)	styrene	ϕ	r/Å	ϵ	σ	ξ/Å	γ	$\omega/10^{-18}$ cm^{-3}	κK	z	N_{sur}	N_{sty}	z/N_{sur}
MEDDAB	5	0	0.046	28.5	1.10		16	180	0.43	2.2	61	144		0.42
MEDDAB	10	0	0.094	29.2	1.16		13	500	0.78	2.4	79	163		0.47
MEDDAB	15	0	0.142	29.8	1.20		15	200	1.02	2.0	50	179		0.28
MEDDAB	15	1.5	0.152	32.0	1.40		16	220	0.79	2.0	53	235	92	0.21
MEDDAB	15	3.0	0.159	34.7	3.40		19	3000	0.27	2.7	194	668	520	0.29
AUTMAB	5	0	0.041	24.8	1.00	0.323	20	24	0.64	1.2	17	105		0.17
AUTMAB	10	0	0.089	25.6	1.00	0.365	20	25	1.27	1.3	18	115		0.15
AUTMAB	15	0	0.137	26.1	1.00	0.362	21	26	1.84	1.2	18	122		0.15
AUTMAB	15	2	0.151	27.1	1.00	0.149	15	21	1.81	1.8	16	120	55	0.14
AUTMAB	15	4	0.161	31.8	1.00	0.140	14	35	1.20	2.3	21	171	159	0.12

[a] Results from computer modeling assuming either polydisperse spheres or monodisperse elliptical particles and a repulsive Yukawa potential. ϕ is the droplet volume fraction, r is the effective droplet radius, ϵ is the minor axis ratio of a prolate ellipsoid, σ is the width of the size distribution function, ξ and γ are the Yukawa interaction parameter, φ is the number density of droplets, κK is the inverse Debye length times the droplet diameter, z is the valence of the single droplet, N_{sur} and N_{sty} are the aggregation numbers of the surfactant and styrene, respectively, and z/N_{sur} is the fraction of dissociated surfactant molecules in the droplet. r, ϵ, σ, ξ, and γ are fit parameters.

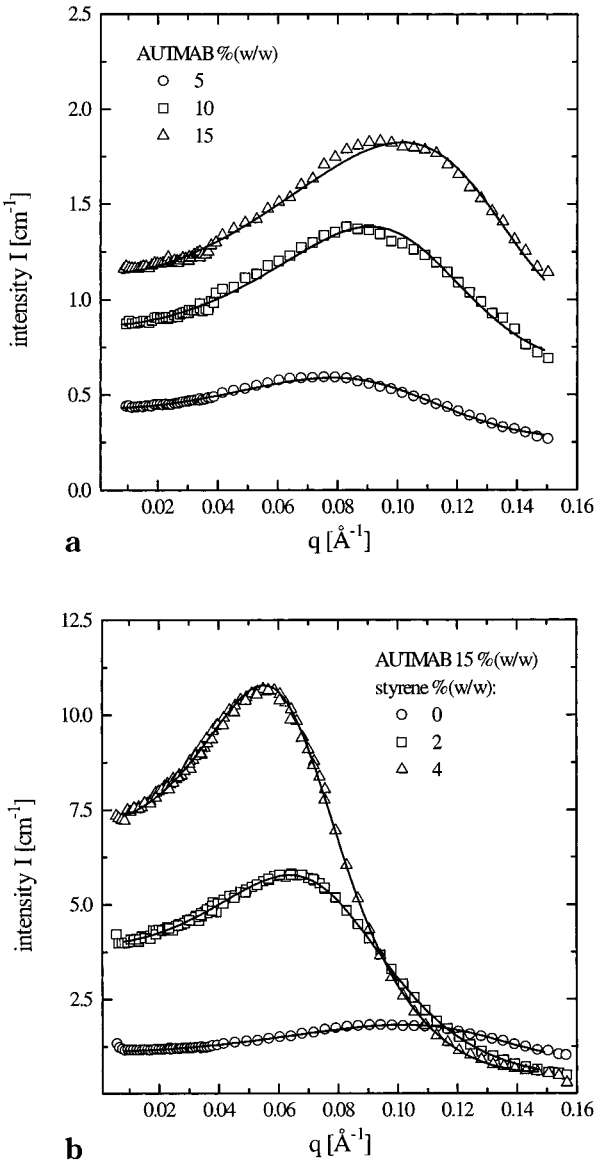

Figure 3. SANS spectra of (a) AUTMAB micelles and (b) microemulsions with styrene at an AUTMAB/water ratio of 15/85% (w/w). Open symbols represent the measured data points, and solid lines are the model intensities.

scattered intensities of the AUTMAB system are much lower, while the characteristic course of the peaks remains the same. For increasing concentration of AUTMAB in micellar solution, the maximum shifts to higher ***q*** values and the absolute scattering intensity increases. In the microemulsion spectra, the maximum intensity distinctly increases, and an analogous shift of the maximum peak position to lower ***q*** values is observed. All scattering data could be best fitted by assuming slightly polydisperse spheres. The modeled parameters are listed in Table 1. The semimajor axis of the AUTMAB micelles in aqueous solution is 25−26 Å, i.e. about 15% smaller than of the MEDDAB micelles. This difference reflects the shorter calculated length of the AUTMAB molecule of approximately 19 Å in its all-trans configuration compared with 23.5 Å for the MEDDAB molecule. In the case of microemulsions with AUTMAB, the addition of styrene leads to an increase of the mean droplet radius until a value of 32 Å is reached for 4% (w/w) styrene in a 15/85 surfactant/water mixture. Here, the modeled polydispersity of the microemulsion droplets is only half the value found for the polydispersity of the pure micelles. Thus one can conclude that the addition of styrene considerably increases the structural order in the solution and that the resulting complex fluid can indeed be considered as an o/w-microemulsion. No change in the axial ratio of the droplets was observed upon styrene addition in contrary to the MEDDAB system, indicating that the oil component does not significantly alter the preferred arrangement of the surfactant molecules in the interfacial layer for the concentration regime investigated here. The apparent micellar charge of the AUTMAB solution is lower compared with the MEDDAB system, indicating a higher degree of gegenion association.

Polymerization. In the following, the results of the γ-ray induced polymerization of the microemulsions are described. After irradiation, the microemulsions are transparent. This contrasts with systems of water/nonpolymerizable surfactant/styrene at comparable styrene content.[6,44] Previous studies on the water/AUTMAB/styrene system using NMR and FTIR spectroscopy as well as elemental analysis have shown that γ-irradiation leads to the formation of a copolymer of styrene and the polymerizable surfactant in a molar ratio of 3:2, while excess surfactant is polymerized by formation of homopolymer.[33] In Table 2, characteristic data of the polymerized microemulsions and their optical appearance are compiled. In the case of AUTMAB, very small and moderately polydisperse latex particles with a core−shell morphology are obtained which are smaller than particles from a DTAB microemulsion of the same concentration. Similar observations have been reported for water/DTAB/styrene microemulsions containing acrylic acid as a comonomer.[17,33] Acrylic acid simultaneously acts as a comonomer and a cosurfactant, which is able to support the stability of the microemulsion during the copolymerization, and this results in smaller particle sizes. Similarly, copolymerized surfactant molecules continuously stabilize the particle shell, which also leads to smaller size.

Table 2. Characteristic Data γ-Ray Induced Polymerization in Different Microemulsion Systems

microemulsion system	monomer composition		appearence of microemulsion		particle size (nm)[a]	σ^b	copolymer composition (mol/mol)
	% (w/w)	mol/mol	before polymer.	after polymer.			
DTAB/styrene	15/4	1.27/1	clear, viscous	turbid, fluid	32.7	0.261	0/1
AUTMAB/styrene	10/2.5	1.15/1	clear, fluid	clear, viscous	19.6	0.546	1/1.5
AUTMAB/styrene	15/4	1.08/1	clear, fluid	clear, viscous	29.5	0.467	
MEDDAB/styrene	5/1	1.29/1	clear, viscous	clear, rigid			
MEDDAB/styrene	10/2	1.29/1	clear, viscous	clear, rigid			1.5/1
MEDDAB/styrene	15/3	1.29/1	clear, viscous	clear, rigid			
MEDDAB/styrene	20/4	1.29/1	clear, viscous	clear, rigid			
MEDDAB/styrene	25/5	1.29/1	clear, viscous	clear, rigid			

[a] Measured by dynamic light scattering. [b] Width of the size-distribution function.

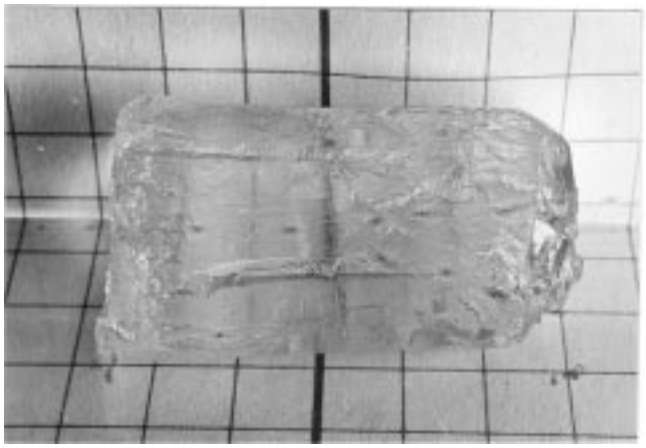

Figure 4. Microemulsion nanogel after γ-irradiation (62 kGy) of the system MEDDAB/styrene 10/2. The size of the sample is 3 × 1.5 cm.

Upon γ-irradiation of the water/MEDDAB/styrene system, rigid transparent polymer gels were obtained. Even samples with a total monomer content of only 6% (w/w) (MEDDAB + styrene) form a gel structure (see Table 2). In Figure 4, a typical microemulsion gel with a water content of about 88% (w/w) is shown. The optical appearance is clear or translucent, similar to microemulsion gels from conventional surfactant, styrene and copolymerized cosurfactant[26] or polymer-bridged and cross-linked networks reported recently.[46] The spectroscopic characterization of the resulting polymer by IR and NMR demonstrates that copolymerization of the oil component and the polymerizable surfactants has taken place. The IR spectra of the two systems show both the vibration bands of the carbonyl units (ν_{co}, 1720 cm^{-1}) and the vibration bands of styrene (aromatic CH and overtones). In Figure 5, the ^{1}H-NMR spectrum of the copolymer obtained from the system water/MEDDAB/styrene 10/2 after γ-irradiation is shown. Because of the amphiphilic nature of the copolymer, the spectrum was recorded at elevated temperature in order to reduce interactions with the solvent dimethylsulfoxide (DMSO). The presence of aromatic protons (**3** (5H) 7.1−7.2 ppm) and the significant signal for the methylene units of MEDDAB (**9** (20 H)) at 1.3 ppm are obvious. Additionally, the CH_3-groups in α-position (**5**, **10** (6 H), 3.1−3.2 ppm) and the CH_2-groups in α-position to the nitrogen and oxygen atoms (**6**, **8** (6H), 3.4−4.3 ppm) can be distinguished. The backbone protons produce broad signals at 1.7−1.9 ppm. The peak integration has been normalized to the aromatic proton signal (5H) and gives a copolymer molar ratio of x being about 2 and y being about 3 in the formula shown in Figure 5. This is in fairly good agreement with the molar ratio of about 1:1 of the starting monomers, especially when the broad NMR signals often found for polymers are regarded. Some uncertainties in the calculation may also be caused by the aggregation behavior of the amphiphilic copolymer in the solvent DMSO-d_6 used for the spectroscopic analysis. Hence it can be concluded that all surfactant monomer has been

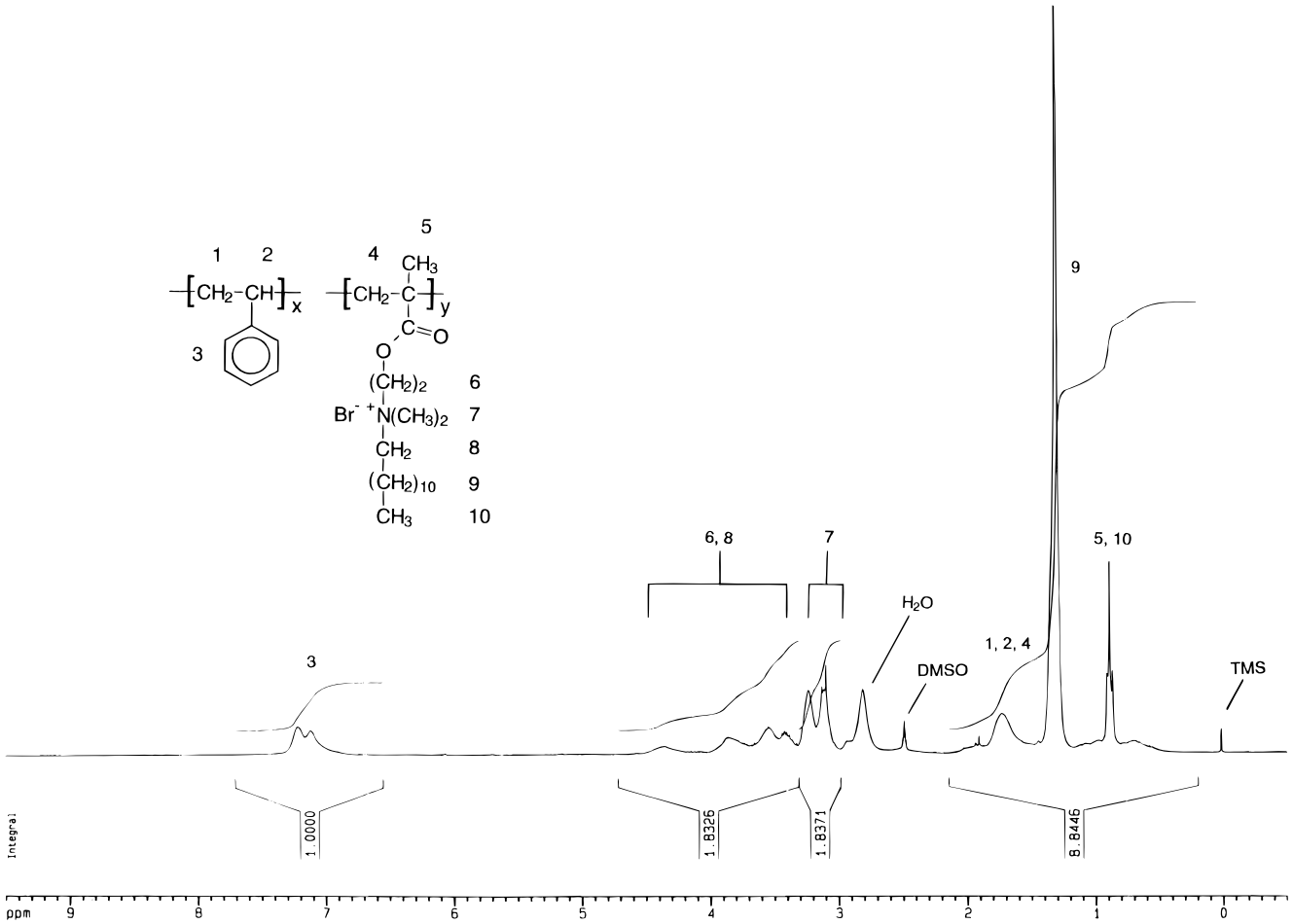

Figure 5. ^{1}H-NMR (300 MHz) spectrum of the copolymer obtained upon γ-irradiation (62 kGy) of the system MEDDAB/styrene 10/2. Spectrum was taken in DMSO-d_6 at 400 K.

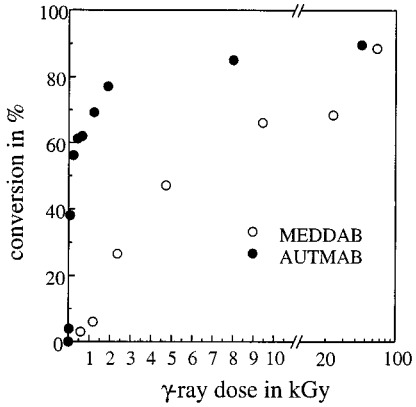

Figure 6. Total conversion vs dose plot for the γ-ray initiated copolymerization of the two systems MEDDAB/styrene 10/2 and AUTMAB/styrene 10/2.5.

incorporated into the copolymer contrary to the AUTMAB/styrene system, where the formation of additional surfactant homopolymer was found.[33]

Conversion vs Dose Behavior. In Figure 6, a conversion vs dose plot is shown for the two microemulsion systems containing either 2 or 2.5% (w/w) styrene in a 10/90 surfactant/water mixture. The conversion denotes the weight percent of both monomers, which are polymerized at a certain γ-ray dose. It is obvious that polymerization of the MEDDAB microemulsion is much slower than of the AUTMAB system. There are two possible reasons for this observation. First, the molecular structure of the H-type surfactant MEDDAB with the reactive methacrylate unit near to the polar headgroup is less favorable for polymerization compared to a T-type surfactant. Second, the position of the reactive unit in the interfacial layer being exposed to the aqueous phase is unfavorable for a copolymerization with the styrene molecules in the hydrophobic core.

The first point has been accounted for by the so-called "skin-controlled solubility" concept.[47,48] T-type surfactants tend to form water-soluble homopolymers with essentially hydrophobic backbone and a hydrophilic outer "surface". Spherical or cylindrical morphologies are prefered, since the ionic headgroups tend to repel each other. H-type surfactants are forced to form homopolymers with a hydrophilic core region and a hydrophobic surface. Regarding the repulsive head groups, the core space is very restricted and thus influences the aggregate shape, which becomes rather disk like or inverse cylindrical in order to minimize the steric demands. This is also important for the understanding of the observed morphological difference between MEDDAB and AUTMAB microemulsions. The second reason is concerned with the probability for copolymerization of the two surfactants with styrene. The polymerizable moiety of a T-type surfactant is in the styrene-filled micellar core, in which the polymerization reaction is supposed to take place. In contrast, the polymerizable moiety of the H-type surfactant is sterically less favorable for an immediate copolymerization with monomer in the core. Thus, in the case of the H-type surfactant, the formation of copolymer with partially polar and nonpolar domains is more likely than for a T-type surfactant. Most recently, the use of similar surfactants in emulsion polymerization has been reported.[49] It turned out that using an T-type surfactant results in very small and monodisperse latices similar to our findings, but the polymerization was very sensitive to the type of initiator used.

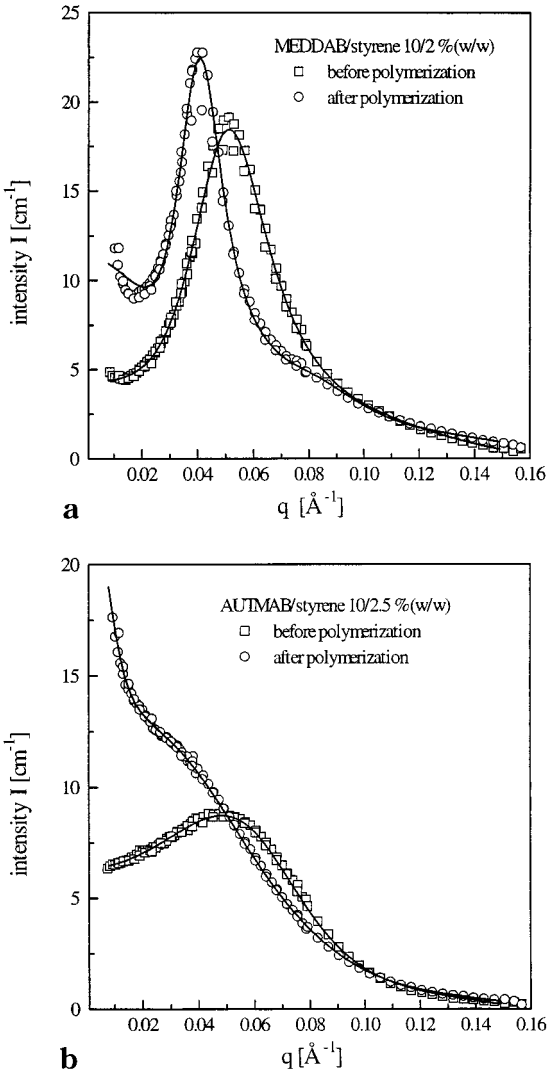

Figure 7. SANS spectra of the microemulsion systems before and after polymerization: (a) MEDDAB and (b) AUTMAB microemulsions at a surfactant/water ratio of 10/90% (w/w). Open symbols represent the measured data points, and solid lines are the model intensities.

Structure Studies after Polymerization. In order to investigate the structural changes during polymerization additional SANS-measurements of the microemulsions after γ-irradiation have been carried out. In parts a and b of Figure 7, the scattering curves are shown together with the calculated intensities. The spectra of the MEDDAB microemulsion before and after polymerization show the characteristic interaction peaks (Figure 7a). After polymerization the maximum is shifted to lower $\boldsymbol{q}$, while the absolute scattering intensity is only slightly increased. This behavior can be interpreted as a growth of the original microemulsion droplets at a simultaneous preservation of the overall structure. The derived fitting parameters are compiled in Table 3. The microemulsion droplets can be best modeled by assuming ellipsoids with a semimajor axis r of 32 Å and a semiminor axis ϵr of about 100 Å. After polymerization, the same elliptical particle form factor is valid, but the ellipsoidal dimensions are enlarged to $r = 43$ Å and $\epsilon r = 150$ Å. It should be pointed out that in the present system, no cross-linker has been used, which is known to favor a preservation of the structures due to conformational entropy reasons.[5] For the

Table 3. Parameters from SANS Spectra Analysis[a]

surfactant	% (w/w)	styrene	ϕ	r/Å	ϵ	σ	ξ/Å	γ	$\varphi/10^{-18}$ cm^{-3}	κK	z	N_{agg}	N_{sty}	z/N_{sur}
MEDDAB	10	2	0.108	32.4	3.14		20	300	0.24	1.4	61	502	391	0.33
MEDDAB	10	2	0.108	43.3	3.47		16	320	0.09	1.5	63			
AUTMAB	10	2.5	0.107	28.8	1.00	0.130	17	35	1.07	1.7	21	129	112	0.16
AUTMAB	10	2.5	0.107	67.6	4.26		53	3	0.02	1.2	6			

[a] For explanation see Table 1.

AUTMAB microemulsion, a significant change in the scattering curves is obvious. The interaction peak of the parent droplet microemulsion disappears and a spectrum with a single, only slightly pronounced peak at lower $\boldsymbol{q}$ appears. Simultaneously, a higher intensity for the $\boldsymbol{q} \rightarrow 0$ region is observed. Here, the model fitting predicts very large elliptical particles. In fact, the size range of particles with a major axis of about 68 Å corresponds quite well with the latex particle size reported earlier,[33] but the semiminor axis of 320 Å is too large to be consistent with results from dynamic light scattering. Here, the scattering intensities may be misinterpreted due to an enhanced polydispersity of the sample or due to particle aggregation, which cannot easily be considered in the model calculations. Nevertheless, we are able to show that a copolymerization of the oil monomer and the surfactant molecules indeed takes place in both systems, since no significant splitting of the microemulsion scattering peak into two separate peaks is observed, as it was reported by Kaler and coworkers for the system water/DTAB/styrene.[20] If the surfactant molecules would only act as nonpolymerizing stabilizers, large latex particles and empty micelles should be formed. In our case, the formation of copolymer latex particles as well as surfactant homopolymer was observed for the AUTMAB system. In the MEDDAB system, the whole monomer forms a nanostructured copolymer gel network which incorporates all the former solvent.

Structure Model. On the basis of our results, a tentative model of the structure formed upon the γ-irradiation of the MEDDAB system has been developed. It is represented in Figure 8b and compared with the corresponding structure model of the AUTMAB system reported previously[33] and shown in Figure 8a. The styrene molecules are located in the droplet cores, in which the polymerization proceeds.[5] If chain growth or an initiation takes place in the droplet shell, the H-type surfactant molecules are sterically more favored for the formation of block structures than for a statistical copolymerization with styrene. Therefore it is likely that polar domains of polymerized surfactant molecules are formed representing polymeric "tentacles" pointing in the aqueous medium which become more and more insoluble during the course of polymerization, and their mobility is reduced. Thus, in the following the chains tend to associate by their hydrophobic tails and the single chains become physically connected. The resulting network structure finally consists of small amorphous polystyrene domains and interpenetrating surfactant polymer chains. In Figure 8a, the proposed mechanism for the copolymerization of a T-type surfactant and styrene in microemulsion is illustrated. The surfactant molecules are preferantially copolymerized with styrene because the reactive tails are adjacent to the droplet cores. Thus, spherical particles are obtained which are electrostatically stabilized and able to grow upon subsequent monomer supply from uniinitiated droplets,[5] so that a core−shell structure results. The

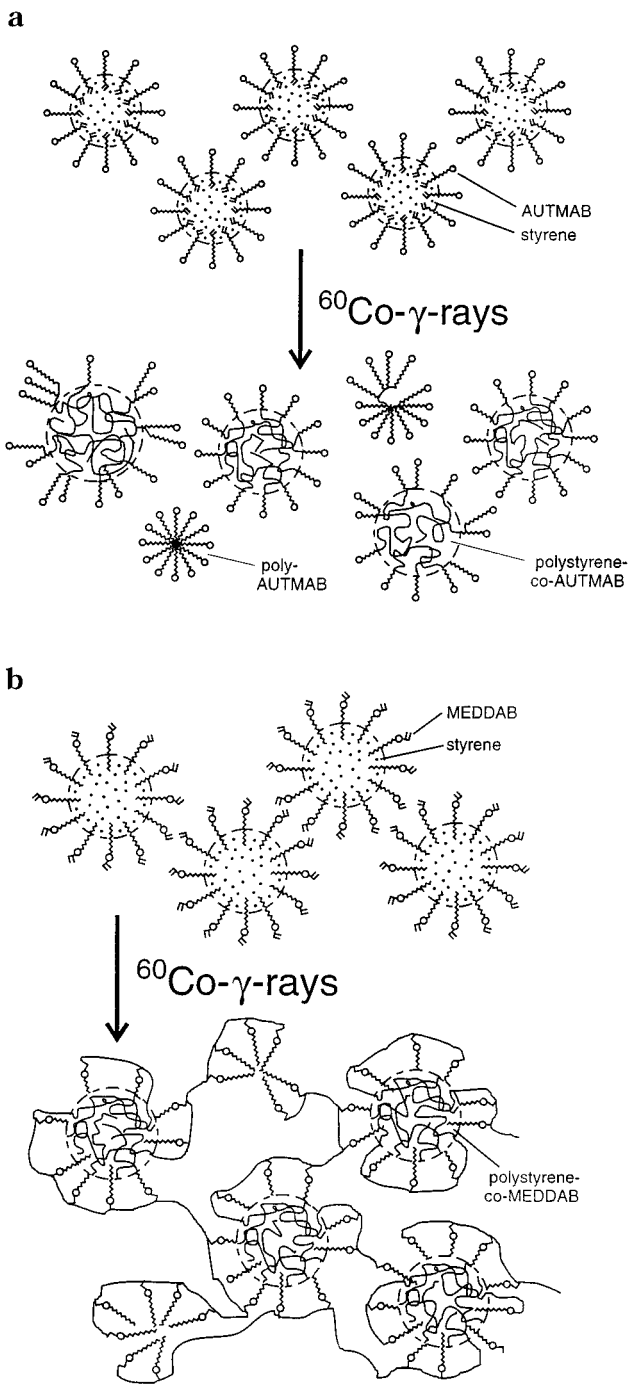

Figure 8. Structure model (not to scale) of a polymerized ternary o/w-microemulsion containing (a) water/AUTMAB/styrene (water/polymerizable T-type surfactant/polymerizable oil) and (b) water/MEDDAD/styrene (water/polymerizable H-type surfactant/polymerizable oil). In part a, core−shell latex nanoparticles are obtained after γ-ray polymerization. In part b, a nanostructured gel is obtained, in which the polymerizable surfactant molecules form an amphiphilic network, whereas polystyrene is located in hydrophobic droplet domains (for details see text).

surplus surfactant molecules polymerize upon further initiation and form styrene-free polymeric micelles.

Summary and Conclusions

Using SANS measurements and spectroscopic methods, we have studied the microstructure and copolymerization behavior of microemulsions containing water, polymerizable surfactant and styrene. It turned out that the molecular structure of the polymerizable surfactant is crucial for the course of the polymerization of the system. Depending on the position of the reactive groups at either the hydrophilic or hydrophobic end of the surfactant, copolymers with different morphology were formed upon γ-ray polymerization of the two systems. In the case of the H-type surfactant MEDDAB, the parent microemulsion structure is largely preserved and a nanostructured copolymer gel is formed, while in the case of AUTMAB redispersible core−shell nanolatex particles are obtained.

It can be concluded that polymerizable surfactants are quite useful in microemulsion polymerization, because the templating effect of the amphiphilic interface can be better preserved during polymerization without the need of any cosurfactant. New materials such as redispersible nanoparticles or highly organized transparent gels with heterogeneities at the nanometer level are obtained. In fact, such highly organized gels exhibiting a large inner surface can be useful as drug delivery systems, as chromatographic resins, or as catalyst carriers. Also, the resulting copolymers themselves are interesting because of their amphiphilic properties. Since the choice of a suitable surfactant for microemulsion formulation is very important, we are still looking for improved surfactant systems which are able to stabilize the (co)polymerization even better.

Acknowledgment. We would like to thank Dr. H. Schmickler, Institut für Organische Chemie, Universität zu Köln, for carrying out the NMR spectroscopy and Prof. Dr. D. Woermann, Institut für Physikalische Chemie, Universität zu Köln, for kindly allowing us to use his tensiometer. M. Behnke of our research group is thanked for taking photographs of the samples.

References and Notes

(1) Sjöblom, J.; Lindberg, R.; Friberg, S. E. *Adv. Colloid Interface Sci.* **1996**, *95*, 125.
(2) Barton, J. *Prog. Polym. Sci.* **1996**, *21*, 399.
(3) (a) Desai, S. M.; Gordon, R. D.; Gronda, A. M.; Cussler, E. L. *Curr. Opin. Colloid Interf. Sci.* **1996**, *1*, 519. (b) Eastoe, J.; Warne, B. *Curr. Opin. Colloid Interf. Sci.* **1996**, *1*, 800.
(4) Candau, F. In *Polymerization in Organized Media;* Paleos, C. M., Ed.; Gordon and Breach Science Publishers: Philadelphia, PA, 1992; p 215.
(5) Antonietti, M.; Basten, R.; Lohmann, S. *Macromol. Chem. Phys.* **1995**, *196*, 441.
(6) Full, A. P.; Kaler, E. W.; Aranello, J.; Puig, J. E. *Macromolecules* **1996**, *29*, 2764.
(7) Gan, L. M.; Chew, C. H.; Lye, I.; Ma, I.; Li, G. *Polymer* **1993**, *34*, 3860.
(8) Stoffer, J. O.; Bone, T. *J. Dispersion Sci. Technol.* **1980**, *1*, 37.
(9) Atik, S. S.; Thomas, J. K. *J. Am. Chem. Soc.* **1981**, *103*, 4279; **1983**, *105*, 4515.
(10) Guo, J. S.; El-Aasser, M. S.; Vanderhoff, J. W. *J. Polym. Sci.: Part A: Polym. Chem.* **1989**, *27*, 691.
(11) Ferrick, M. R.; Murtagh, J.; Thomas, J. K. *Macromolecules* **1989**, *22*, 1515.
(12) Perez-Luna, V. H.; Puig, J. E.; Castano, V. M.; Rodriguez, B. E.; Murthy, A. K.; Kaler, E. W. *Langmuir* **1990**, *6*, 1040.
(13) Antonietti, M.; Bremser, W.; Müschenborn, D.; Rosenauer, C.; Schupp, B.; Schmidt, M. *Macromolecules* **1991**, *24*, 6636.
(14) Puig, J. E.; Perez-Luna, V. H.; Perez-Gonzales, M.; Macias, E. R.; Rodriguez, B. E.; Kaler, E. W. *Colloid Polym. Sci.* **1993**, *271*, 114.
(15) Gan, L. M.; Chew, C. H.; Lim, J. H.; Lee, K. C.; Gan, L. H. *Colloid Polym. Sci.* **1994**, *272*, 1082.
(16) Schubert, K.-V.; Lusvardi, K. M.; Kaler, E. W. *Colloid Polym. Sci.* **1996**, *274*, 875.
(17) Puig, J. E.; Corona-Galvan, S.; Maldonado, A.; Schulz, P. C.; Rodriguez, B. E.; Kaler, E. W. *J. Colloid Interface Sci.* **1990**, *13*, 7308.
(18) Antonietti, M.; Lohmann, S.; Van Niel, C. *Macromolecules* **1992**, *25*, 1139.
(19) Antonietti, M.; Lohmann, S.; Eisenbach, C. D.; Schubert, U. S. *Macromol. Rapid Commun.* **1995**, *16*, 238.
(20) Larpent, C.; Bernard, E.; Richard, J.; Vaslin, S. *Macromolecules* **1997**, *30*, 354.
(21) Palani Raj, W. R.; Sasthav, M.; Cheung, H. M. *Langmuir* **1991**, *7*, 2586.
(22) Palani Raj, W. R.; Sasthav, M.; Cheung, H. M. *Polymer* **1995**, *36*, 2637.
(23) Chieng, T. H.; Gan, L. M.; Chew, C. H.; Lee, L.; Ng, S. C.; Pey, K. L.; Grant, D. *Langmuir* **1995**, *11*, 3321
(24) Chieng, T. H.; Gan, L. M.; Chew, C. H.; Ng, S. C., Pey, K. L. *J. Appl. Polym. Sci.* **1996**, *60*, 1561.
(25) Burban, J. H.; He, M.; Cussler, E. L. *AIChE J.* **1995**, *41*, 159.
(26) Antonietti, M.; Hentze, H.-P. *Colloid Polym. Sci.* **1996**, *274*, 696.
(27) Chieng, T. H.; Gan, L. M.; Chew, C. H.; Ng, S. C.; Pey, K. L. *Polymer* **1996**, *37*, 2801.
(28) Chieng, T. H.; Gan, L. M.; Teo, W. K.; Pey, K. L. *Polymer* **1996**, *37*, 5917.
(29) Palani Raj, W. R.; Sasthav, M.; Cheung, H. M. *Langmuir* **1992**, *8*, 1931.
(30) Li, T. D.; Chew, C. H.; Ng, S. C.; Gan, L. M.; Teo, W. K.; Gu, J. Y.; Zhang, G. Y. *J. Macromol. Sci.—Pure Appl. Chem* **1995**, *A32*, 969.
(31) Gan, L. M.; Li, T. D.; Chew, C. H.; Teo, W. K.; Gan, L. H. *Langmuir* **1995**, *11*, 3316.
(32) Hammouda, A.; Pileni, M.-P. *Langmuir* **1995**, *11*, 3656.
(33) Dreja, M.; Tieke, B. *Macromol. Rapid Commun.* **1996**, *17*, 825.
(34) Nagai, K.; Okishi, Y.; Inaba, H.; Kudo, S. *J. Polym. Sci.: Polym. Chem. Ed.* **1985**, *23*, 1221.
(35) Hamid, S. M., Sherrington, D. C. *Polymer* **1987**, *28*, 325.
(36) Hayter, J. B.; Penfold, J. *Colloid Polym. Sci.* **1983**, *261*, 1022.
(37) Chen, S.-H. *Annu. Rev. Phys. Chem.* **1986**, *37*, 351.
(38) Kotlarchyk, M.; Chen, S.-H. *J. Chem. Phys.* **1983**, *79*, 2461.
(39) Perdersen, J. S. *J. Appl. Cryst.* **1994**, *27*, 595.
(40) D'Aguanno, B.; Klein, R. *J. Chem Soc., Faraday Trans.* **1991**, *87*, 379.
(41) Hayter, J. B.; Penfold, J. *Mol. Phys.* **1981**, *42*, 109.
(42) Pedersen, J. S. *Lecture notes for The Third European Summer School on "Scattering Methods Applied to Soft Condensed Matter"*; 1996.
(43) (a) Berr, S. S.; Coleman, M. J.; Jones, R. R. M.; Johnson, J. S., Jr. *J. Phys. Chem.* **1986**, *90*, 6492. (b) Berr, S. S. *J. Phys. Chem.* **1987**, *91*, 4760.
(44) Full, A. P.; Kaler, E. W. *Langmuir* **1994**, *10*, 2929.
(45) Imae, T. *Colloids Surf. A* **1996**, *109*, 291.
(46) Meier, W. *Langmuir* **1996**, *12*, 6321.
(47) Aoki, S.; Morimoto, Y. *Polym. Bull.* **1996**, *37*, 777.
(48) Laschewski, A. *Adv. Polym. Sci.* **1995**, *124*, 1.
(49) Cochin, D.; Laschewski, A.; Nallet, F. *Macromolecules* **1997**, *30*, 2278.

MA971153I